ELSEVIER

Journal of Molecular Catalysis A: Chemical 106 (1996) 241–254

JOURNAL OF MOLECULAR CATALYSIS A: CHEMICAL

Surface characteristics and catalytic activity of Al-Pillared (AZA) and Fe–Al-pillared (FAZA) clays for isopropanol decomposition

A.K. Ladavos, P.N. Trikalitis, P.J. Pomonis *

Department of Chemistry, University of Ioannina, 45332, Ioannina, Greece

Received 27 April 1995; accepted 25 September 1995

Abstract

Fractionated Al-pillared (code name AZA) and Fe–Al-pillared (code name FAZA) clays were examined for the dependence of their specific surface area on the particle size. The results indicate a very weak dependence and a fractal dimension of $D \approx 3$ for both materials, characteristic of highly porous solids. The a_s plots of the fractionated particles show that the part of the surface area due to the mesoporosity plus the external surface, decreases as the particle size increases and possess a fractal dimension equal almost to 2.8. For both kinds of solids, AZA and FAZA as well as zeolite-Y, the acidity estimated by NH_3 adsorption was found equal to 1.4×10^{18}, 2.2×10^{18} and 2.1×10^{18} sites per m^2 respectively. The experimental results of catalytic activity of AZA, FAZA and zeolite-Y, using the decomposition of isopropanol as a probe reaction in the range of 60 to 130°C, suggest that AZA is catalytically more active compared to FAZA for the total conversion of isopropanol. The reaction rate calculated per g is one order of magnitude higher on the zeolite-Y, as compared to AZA and/or FAZA, due to its higher surface area but it is almost equal if the comparison is made per unit surface area. The products obtained were mainly propene and diisopropyl ether with a selectivity for propene laying between 0.8–0.9 irrespective of particle size of the solids or the temperature. On the contrary, zeolite-Y shows a high selectivity for propene (≈ 0.9) only at low conversions while at higher conversion selectivity tends to 0.5. The kinetic investigation of the reaction showed single Arrhenius plots for AZA and zeolite-Y with apparent activation energies (E_{app}) around 80–90 kJ/mol for AZA and 70 kJ/mol for zeolite. On the contrary, FAZA showed two distinct regions in the Arrhenius plots. One at low temperatures ($T < 100$°C) with E_{app} 25–35 kJ/mol and another at high temperatures ($T > 100$°C) with $E_{app} \approx 70$–80 kJ/mol, depending on the fraction of the solid. This alternation of catalytic behaviour in FAZA was attributed to the extensive adsorption of water at higher conversions that leads to kinetic expression inhibited by the adsorbed water, while at lower conversions first order kinetic is proposed. AZA on the other hand as well as zeolite-Y shows kinetic behaviour inhibited by water adsorption even at very low conversions.

Keywords: Pillared clays; Zeolite-Y; Isopropanol; Decomposition

1. Introduction

Sixty years ago, Eugene Houdry found that acid-modified smectites provided gasoline in high yield when used as petroleum-cracking catalysts [1]. These modified clays were used extensively as

* Corresponding author. Tel. (+30-651) 98361, fax, (+30-651) 44836.

SSDI 1381-1169(95)00281-2

commercial catalysts until the mid-60's, when they were replaced by more thermally stable and selective zeolites. Smectite clays of natural origin are layered alumino-silicates which are held together by weak electrostatic forces. Recent advances in the intercalation chemistry of smectite clays have provided interest in these minerals as catalysts or catalyst supports. The first preparations used tetralkylammonium ions [2] and yielded expanded clays which could act as molecular sieves for adsorption of organic molecules. However, the low thermal stability of these organic clays limited their applications to catalysis. New classes of materials have recently been developed by preparation of pillared interlayered clays with polyoxocations stable up to 500–600°C. Inorganic polymeric metal cations derived from water soluble salts or complexes of aluminium [3–5], iron [6], chromium [7], zirconium [8] and nickel [9] appear to be the most widely explored pillared agents. To date, clays intercalated with monometallic pillars have received primary attention. However there are some papers which report the preparation of pillared clays with mixed-metal complexes or mixed polycations [10,11].

Microporous networks created in the interlayer region of clays after pillaring provide pore-size distributions of extended range (0.6–4.0 nm) compared to those found within typical zeolites (0.2–0.8 nm) [12]. Aluminium pillared clays therefore, have been evaluated as potential catalysts for treatment of large hydrocarbon molecules in reactions like Friedel–Crafts alkylation, disproportionation, isomerization and other similar routes which are catalysed by acid centres. Major difficulties exist, however, as these materials are unstable at industrial reaction temperatures. An additional reason that pillared clays have not been applied as industrial catalysts up to now is that they have not been prepared reproducibly in large quantities.

This work deals with two pillared clays, an aluminium pillared clay, code name AZA and an iron–aluminium pillared clay, code name FAZA. Those materials have been prepared at kilogram quantities and have been accepted by the participants as internal reference materials in a 'Coordinated European Activity on Pillared Layered Structures' (CEA–PLS) [13]. The readers interested in the subject can also consult a relevant collective publication [14] containing a wealth of information on this subject. The aim of this study is to characterise the pore structure, the acidic and the catalytic properties of such solids. Pillared clay catalysts should be active for acid catalysed reactions like the decomposition of isopropanol. This reaction has been extensively used as a probe reaction in order to test the catalytic activity of various acid solids [15–18]. The use of zeolite-Y was decided in order to have a comparison of these AZA and FAZA novel solids with an established catalyst.

2. Experimental

2.1. Materials

The pillared clays AZA and FAZA used in this work have been prepared by Straton Hi Tec Ltd., Athens, Greece [13]. They are based on the clay mineral montmorillonite (brand Zenith) which originated in the Greek island of Milos. The first pillared clay AZA is only aluminium pillared montmorillonite while the second one termed FAZA is pillared by iron plus aluminium in a 50% ratio located in the same pillar, as revealed by a recent detailed Mössbauer study [19]. The data sheet of the solids provided by the producer gives the following information: $ssa_{AZA} = 225 \pm 10$ m^2 g^{-1}, $ssa_{FAZA} = 240 \pm 10$ m^2 g^{-1}, d-space$(001)_{AZA} = 1.82 \pm 0.02$ nm and d-space$(001)_{FAZA} = 1.83 \pm 0.03$ nm. Before the experiments the as-received materials were sieved to six different particle sizes between 200 and 1000 μm. For both materials the fractions obtained were: 200–250 μm, 250–425

μm, 425–500 μm, 500–600 μm, 600–710 μm and 710–1000 μm. All the experiments and comparisons were carried out for three fractions 200–250 μm, 425–500 μm, and 710–1000 μm. The zeolite used in this work was commercial LZ-Y62 from Linde of particle size 1–5 μm.

2.2. Specific surface area measurements

The surface areas and pore volumes of the samples were determined with a volumetric adsorption–desorption apparatus, using Nitrogen as adsorbent at 77 K. Prior to the determination of the adsorption isotherms the samples were degassed at 250°C under 5×10^{-3} mbar vacuum for 18 h. The specific surface area determination of the samples was accomplished by applying the BET equation using only the linear part ($0.05 < P/P_0 < 0.25$) of adsorption isotherm and assuming a close-packed BET monolayer, with $a_m(N_2) = 0.162$ nm^2 at 77 K. The evaluation of microporosity and the mesoporosity plus the external area of AZA and FAZA was carried out by the a_s plot method [20,21]. Furthermore with the same method we calculated the microporous volume of the above materials.

2.3. Surface acidity measurements

The temperature programmed desorption (TPD) of ammonia was used to evaluate the total (Lewis + Brønsted) surface acidity of our materials [22]. A sample weighing about 0.5 g, was put in a silica tube having a perforated-glass silica tube. The tube was connected to a Gas Chromatograph Varian 3700 with a TC detector. Each sample was initially heated at 500°C in a flow of helium for 2 h, after which the temperature was reduced to the working level 100°C, at which the sample was saturated with dried ammonia (Merck, water-free, 0.2% water). This operation was carried out by replacing, for 30 min, the flow of Helium through the sample, by a flow of dried ammonia. Then the weakly adsorbed ammonia was flushed out with Helium (30 ml/min) for 2 h at 110°C. After removal of the weakly adsorbed ammonia the sample was cooled to 100°C and programmed heating begun at a rate 3°C/min till 500°C where it remained for 2 h. A preliminary calibration of the TC detector of the GC with respect to eluted ammonia made it possible to determine it from the areas of the peaks on the TPD curves. The amount of ammonia eluted was also trapped in a bubble bottle which contains an excess of 0.01 N hydrochloric acid solution. Then the trapped NH_3 was evaluated by volumetric determination of the excess HCl using 0.01 N NaOH.

2.4. Isopropanol decomposition

The catalytic decomposition of isopropanol took place in a bench-scale flow reactor, similar to that described in refs. [15,16]. The reactor consisted of a silica tube 1 cm in diameter with a sealed-in quartz bed onto which 0.5 g of the catalyst was placed. The system was heated in a tubular furnace with a control system to within ±1°C. Analyses of reactants and products were carried out by sampling 1 cm^3 of the gasses in a Shimadzu GC-15A gas chromatograph equipped with a thermal conductivity detector and connected to a Chromatopac C-R6A integrator. The column used for analysis was 2 m × 1/8 in. s.s., 10% Carbowax 20M on Chromosorb W-HP, 80–100 mesh. Helium was used as carrier gas in the gas chromatograph. Another line drove Helium through a saturator bottle (40 ± 1 cm^3 min^{-1}) containing the isopropanol, whose vapour was then driven to the reactor. Under the experimental conditions the partial pressure of isopropanol was 32.82 mmHg. Measurements were taken randomly in the range of 60 to 130°C in 5°C intervals. Before the catalytic

experiments were started AZA and FAZA solids were heated at 200°C for 2 h under Helium flow and the zeolite was heated at 420°C in Helium flow for 3 h to remove adsorbed water from the pores. No signs of catalyst 'die off' were observed during the time scale of our experiments. The products detected were propene and diisopropyl ether. From the percentage degree of total conversion of isopropanol we calculated the reaction rate at each reaction temperature. Moreover the selectivity for each main product propene and diisopropyl ether at various degrees of total conversion of isopropanol was also found.

3. Results

3.1. Surface area – pore volume – a_s plots

The N_2 adsorption–desorption isotherms for three different fractions (200–250 μm, 425–500 μm, and 710–1000 μm) of the AZA and FAZA materials are shown in Fig. 1.

The results of the BET specific surface areas as well the pore volumes of the checked samples as well as LZ-Y62 zeolite are reported in Table 1. From the adsorption isotherms that are shown in Fig. 1 it is possible to estimate the a_s plots of the solids. The a_s plots, defined as $a_s(n/n_s)_{ref}$ (n_s is the amount adsorbed by the reference solid at $P/P_0 = s$) has been proposed [20,21] as a very valuable tool to investigate the porosity of the solids. According to Gregg and Sing [20] it is convenient to place $a_s = 1$ at $P/P_0 = 0.4$, since monolayer coverage and microporous filling occur at $P/P_0 < 0.4$, while capillary condensation takes place at $P/P_0 > 0.4$. By plotting for a test sample the nitrogen volume, V, adsorbed at a relative pressure, P/P_0, as a function of the a_s value from the reference

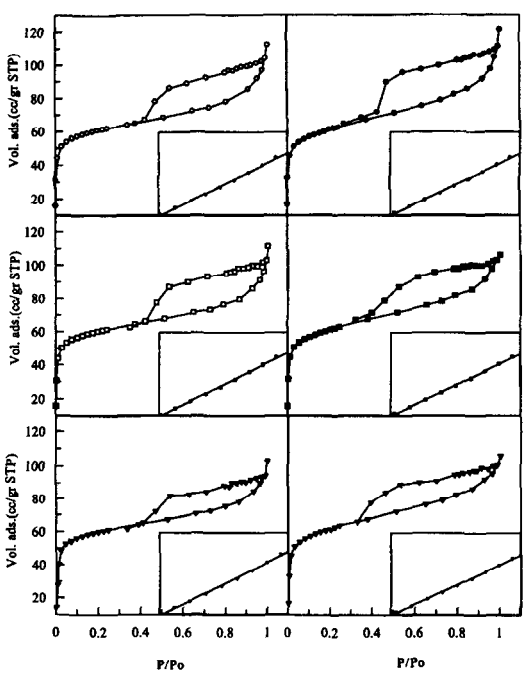

Fig. 1. Adsorption–desorption isotherms of the three fractions (○,●, 200–250 μm; □,■, 425–500 μm and ▽,▼, 710–1000 μm) of AZA (open symbols) and FAZA (filled symbols). The inserts show the BET plots.

Table 1
Particle sizes, surface areas (total, external plus mesoporous and microporous) and pore volume of the solids AZA and FAZA. The particle size of zeolite LZ-Y62 and its surface area are also shown

Sample	Particle size (μm)	Total surface area (m^2/g)	Total pore volume (cm^3/g)	External + meso surface area (m^2/g)	Micro surface area (m^2/g)	Microporous volume (cm^3/g)	% Micro surface area
AZA	200–250	202	0.132	53	149	0.083	74
	425–500	201	0.133	53	148	0.079	74
	710–1000	196	0.131	46	150	0.084	76
FAZA	200–250	205	0.142	61	144	0.082	70
	425–500	205	0.142	55	150	0.086	73
	710–1000	207	0.148	41	166	0.100	80
LZ-Y62	1–5	940					

material at the corresponding P/P_0, valuable information can be obtained about the porous structure of the adsorbent. In the present work Na-montmorillonite was used as reference material. At low relative pressures (low a_s values) the slope of V–a_s plot gives the surface area. At higher relative pressures (higher a_s values), deviations of the straight line might occur. An upward deviation indicates that mesoporosity has been introduced while a downward deviation is observed when micropores or slit-shaped pores are present. In the second case, the positive intercept gives the microporous volume, $V_{\mu p}$, after conversion of the gas volume adsorbed at 77 K ($V_{\mu p} = V_{ads}(STP) * 0.001547$) while the slope gives the meso + external surface area $S_{m,e}$ ($S_{m,e} = 2.87 * V_{ads}/a_s$).

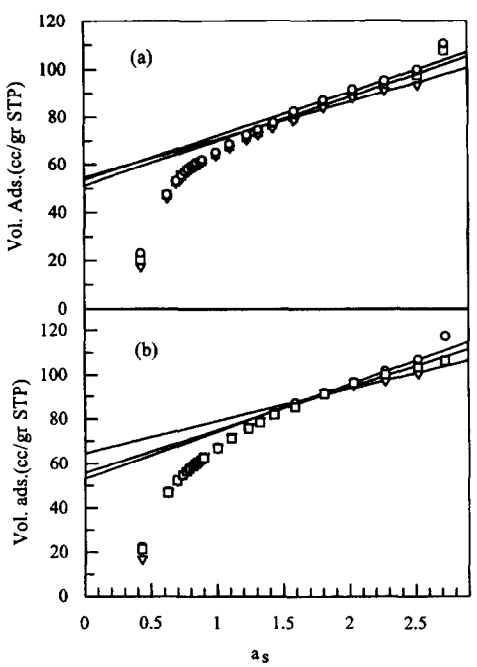

Fig. 2. a_s plots for the three observed fractions of (a) AZA and (b) FAZA (○, 200–250 μm; □, 425–500 μm and ▽, 710–1000 μm).

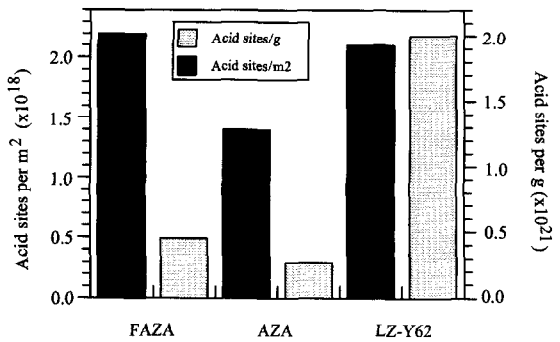

Fig. 3. Acid sites per g and per m^2 of AZA and FAZA solids (710–1000 μm fraction). Data for zeolite-Y are included for comparison.

The a_s plots of the three fractions of AZA and FAZA are shown in Fig. 2. The calculated values of meso + external, surface area as well as the microporous surface area and microporous volume calculated as described above are reported in Table 1.

3.2. Surface acidity

The number of acid sites for AZA (710–1000 μm fraction), FAZA (710–1000 μm fraction) and zeolite-Y (LZ-Y62) per g as well as per m^2 are shown in the histogram of Fig. 3.

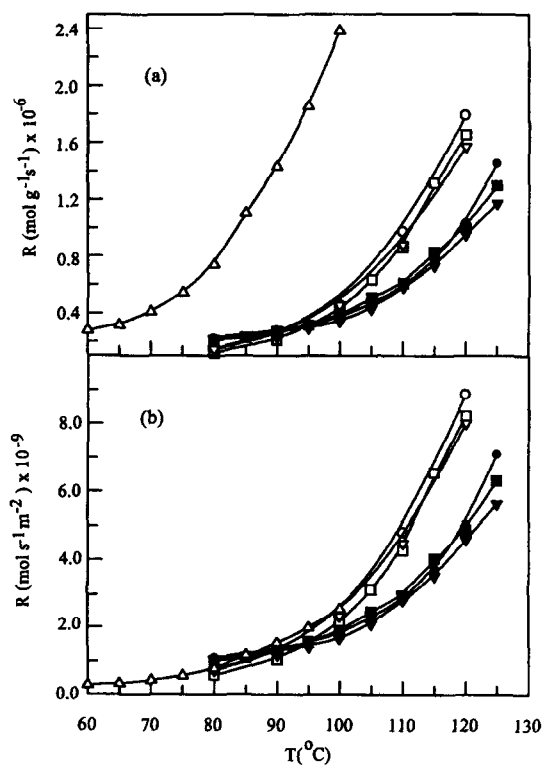

Fig. 4. Reaction rates versus temperature calculated (a) per g or (b) per m^2 of the three observed fractions (○,●, 200–250 μm; □,■, 425–500 μm and ▽,▼, 710–1000 μm) of AZA (open symbols) and FAZA (filled symbols). The data from zeolite-Y are also shown for comparison (△).

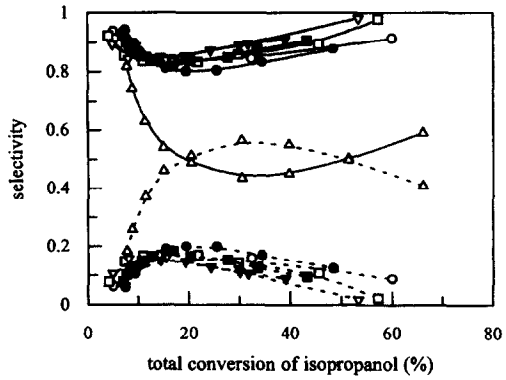

Fig. 5. Selectivities for the production of propene (solid lines) and diisopropyl ether (dashed lines) (○,●, 200–250 μm; □,■, 425–500 μm and ▽,▼, 710–1000 μm) of AZA(open symbols), FAZA (dark symbols) and Zeolite-Y (△).

In order to estimate the total number of acid sites we consider that every molecule of NH_3 occupies one acid surface site. It can be seen that the number of acid sites of AZA, FAZA and zeolite-Y evaluated from NH_3 adsorption is almost equal if calculated per m^2. However the acidity per unit mass for the zeolite-Y is one order of magnitude higher as compared to that of pillared clays. This fact is due to the higher surface area of zeolite-Y (940 $m^2\ g^{-1}$) which is 4.5 times higher as compared to that of AZA and FAZA ($\approx 200\ m^2\ g^{-1}$).

3.3. Isopropanol decomposition

The calculated catalytic activity of the solids is shown in Fig. 4 in the form of the rate of total isopropanol conversion calculated either per unit mass (R/mol $g^{-1}\ s^{-1}$) or per unit area (R/mol $m^{-2}\ s^{-1}$) of the catalysts as a function of reaction temperature.

The calculated selectivities for propene and diisopropyl ether are also shown in Fig. 5.

4. Discussion

4.1. The fractality of AZA and FAZA

The pillared layered materials, as the ones examined in this work, are considered as having porosity due to minute pillars stabilised between the aluminosilicate layers. Apart from this internal porosity, it is possible to have some kind of external porosity due to the agglomeration of aluminosilicate pillared particles. A first important question for such materials is if their porosity is truly isomorphous and three dimensional or if there is a preference towards two dimensional structures. An answer to such questions can be addressed by calculating the well-known fractal dimensionality of such solids [23–25]. Since the details of this theory are by now well known it is enough to state here that there are two methods usually employed for calculating the fractal dimensionality of a solid surface [24,25]. The first is based on adsorption of small molecules of increasing cross-sectional area σ and measurement of surface A accessible for each one of them. The smallest molecule usually employed is N_2 (16.2 $Å^2$) while the largest are dye molecules (100–200 $Å^2$). Then

$$A \propto \sigma^{(2-D)/2} \tag{1}$$

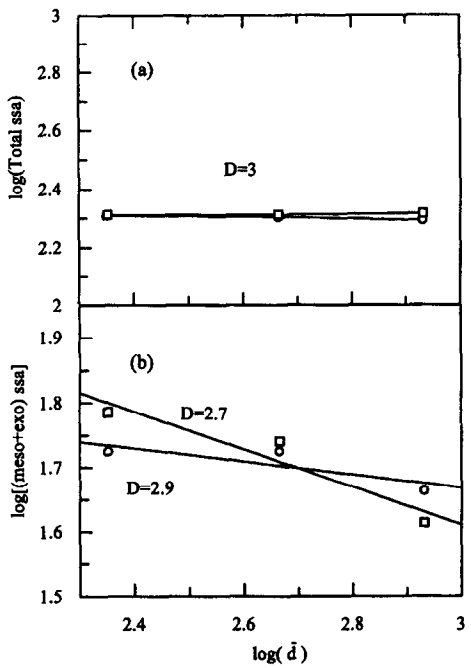

Fig. 6. Plots of log(ssa) = f(log($\bar{d}$)) for the estimation of fractal dimension of (○) AZA and (□) FAZA. (a) Data referred to the total surface area; (b) data referred to the external surface area (exo) plus the area due to mesoporosity (meso) as observed in Table 1.

where D is the fractal dimensionality of the surface accessible for adsorption of molecules of successive size.

According to the second method, adsorption of a single molecule – usually N_2 – takes place on particles of successively increasing size, d. Then

$$A \propto d^{D-3} \tag{2}$$

Eq. (2) in its logarithmic form $\log A \propto (D-3)\log d$ can easily provide the values of D assuming enough A and d input information. This second approach was followed in the present study as shown in Fig. 6.

In this figure the logarithm of the total surface area from Table 1 as well as that of the surface area due to mesoporosity plus external surface (as found from the a_s plots and tabulated in Table 1) have been plotted versus the logarithm of the mean particle size of the three tested fractions of AZA and FAZA. The results obtained using the total surface area suggest for both materials $D \approx 3$. This value indicates a highly porous material with isomorphous distribution of its porosity into space. The results obtained using the mesoporosity plus the external surface area, suggest a fractal dimension slightly lower and around 2.9 for AZA and 2.7 for FAZA. This result suggests that the mesoporous surface area created by the agglomeration of pillared particles, and which is actually the largest part of the sum (meso + exo), is seen as not quite isomorphous by the adsorbed species but indeed as having a two dimensional distribution. We recall that the bulk of work on examining the fractal dimension of clays or pillared clays has been done by Van Damme and co-workers [26,27]. They have found values of $D \approx 2$ for Al_{13} pillared montmorillonite, 1.9 for montmorillonite as well as hectorite pillared with various alkyloammonium cations [26] but they found $D = 2.47–3.00$ for cation exchanged montmorillonite [27]. In this last case also the appearance of values of D approaching 3 indicates that the adsorption of cations takes place isomorphically in a three dimensional porous solid and not just on or

between the lamellae. This might be due to the existence of particles which at larger sizes (as those examined in the present work or in ref. [27]) appear as three dimensional, but consist of two-dimensional microdomains. If this suggestion is correct then examination of particles smaller than 200 μm could reveal the two-dimensionality of AZA and FAZA, which is an object of future examination.

4.2. Acidity

The total acidity (Brønsted and Lewis) of AZA and FAZA as determined by NH_3 adsorption appears higher on FAZA as compared to AZA both per unit mass (g) as well as per unit surface (m^2). In comparison to zeolite-Y these materials possess fewer acid sites per g, but the surface acid density is almost similar (see Fig. 3). Especially FAZA appears to possess even greater surface density of total acid sites than zeolite-Y. The average surface area corresponding to each acid site is 45 $Å^2$/site for FAZA, 70 $Å^2$/site for AZA and 47 $Å^2$/site for zeolite-Y. Nevertheless an important feature of the acidity is that it does not result in similar reaction products. Namely AZA and FAZA yield mainly propene while zeolite-Y yields propene and diisopropyl ether in almost equal quantities (see Fig. 5). This means that it is not only the density but also the strength of acid sites that influences the final products. We notice for comparison that in a previous work [16] referred to La-pillared montmorillonite the surface acid density was found almost similar (1.3 to 3.6×10^{18} sites/m^2) while the dehydrating behaviour of those solids was also solely towards propene.

4.3. Isopropanol transformation – mechanism and kinetics

The main product obtained both on AZA as well as on FAZA during the transformation of isopropanol is propene with a selectivity around 0.9 for degrees of conversion $40\% < x < 10\%$ and 0.8 for $40\% > x > 10\%$ (see Fig. 5). The other product obtained was diisopropyl ether. No sign of acetone was observed. There is not any appreciable differentiation of the products obtained on the different fractions of particles between AZA or FAZA. On the contrary, zeolite-Y is strongly differentiated, as compared to AZA and FAZA, and provides propene and diisopropyl ether almost in equal selectivities 0.5 especially at conversions higher than 10%. These observations lead to the conclusion that the acid sites responsible for the dehydration in pillared clays and zeolites are not of similar kind, resulting in dissimilar products.

As far as the kinetics of the reaction concern, we consider in a first approach 1st order kinetics, which is the simplest and most common treatment applied to this reaction [15,28–32]

$$R = k\theta_{C_3H_8O} \tag{3}$$

Assuming Langmuirian adsorption isotherms we obtain

$$\theta_{C_3H_8O} = \frac{b_{C_3H_8O} P_{C_3H_8O}}{1 + \sum k_i P_i} \tag{4}$$

where b, P – have their usual meaning, i – corresponds to all the reactants and products of the reaction (5) which are isopropanol, propene, diisopropyl ether, helium and water, and correspond to the moles shown in Eq. 5.

$He + C_3H_8O$	$\rightarrow$	He	+	C_3H_8O	+	C_3H_6	+	$C_6H_{14}O$	+	H_2O
Final moles:		n_o		$n(1-x)$		ny		$n\frac{z}{2}$		$ny + n\frac{z}{2}$

(5)

where n_0 is number of moles of He in the feed, n number of moles of isopropanol in the feed at zero conversion, x is the total degree of conversion of isopropanol, y the degree of conversion to propene, and z the degree of conversion to diisopropyl ether: $x = y + z$. Then assuming weak adsorption of all the reactants and products ($1 \gg \sum k_i P_i$), Eq. (4) obtains the form

$$\theta_{C_3H_8O} = b_{C_3H_8O} P_{C_3H_8O} \tag{6}$$

and Eq. (3) becomes

$$R = k b_{C_3H_8O} P_{C_3H_8O} \tag{7}$$

Then expressing the partial pressure of isopropanol as a function of its initial pressure $P^{\circ}_{C_3H_8O}$, of the degrees of conversion x and y and the total pressure in the reactor P_t, we obtain after lengthy but rather trivial transformations

$$R = k b_{C_3H_8O} \frac{(1-x) P^{\circ}_{C_3H_8O}}{y P^{\circ}_{C_3H_8O} + P_t} P_t \tag{8}$$

We can now make use of the so called design-equation of the plug flow reactor, as the one used in our case [15,33,34]

$$F\,dx = R\,dS \tag{9}$$

where F is the feed (moles/s) and S the surface area of the catalyst. Substitution of Eq. (8) into (9) and integration yields

$$-\alpha x - \left(\alpha + \frac{P_t}{P^{\circ}_{C_3H_8O}}\right) \ln(1-x) = \frac{k b_{C_3H_8O}}{F} S P_t \tag{10}$$

where α is the selectivity of propene. For $P_t = 720$ mmHg, $P^{\circ}_{C_3H_8O} = 32.82$ mmHg as in our experiment we can easily rearrange Eq. (10) in the form

$$\ln[-\alpha x - (21.94 + \alpha)\ln(1-x)] = -\frac{E_{app}}{R}\frac{1}{T} + \ln\left[\frac{A S P_t}{F}\right] \tag{11}$$

where $k = A\exp(-E_{app}/RT)$, E_A is the true activation energy of reaction, $b_{C_3H_8O} = \exp[(-\Delta H_{C_3H_8O})/RT]$, $-\Delta H_{C_3H_8O}$ is the enthalpy of adsorption of isopropanol and E_{app} is the apparent activation energy of the process related to E_A and ΔH by the relationship $E_{app} = E_A - \Delta H_{C_3H_8O}$.

Then plots of the left hand part of Eq. (11) versus $1000/T$ can be used to obtain the apparent activation energy of the reaction E_{app}. Such plots are shown in Fig. 7. The calculated numerical values of E_{app} are included in Table 2.

From the Arrhenius drawn in Fig. 7 it is immediately apparent that the FAZA catalysts behave differently, indicating two regions of activation energy: The first appears at higher temperatures ($T > 100$°C) and higher conversions where E_{app}(FAZA) equals 78.6, 69.5 and 70.7 kJ/mol for the three fractions 200–250 μm, 425–500 μm, and 710–1000 μm respectively. The second region appears at lower temperatures ($T < 100$°C) and lower degrees of conversion. There E_{app}(FAZA) equals 28.1, 36.5 and 25.2 kJ/mol for the three particle fractions. We also notice that the E_{app} calculated for AZA are 83.8, 89.5 and 79.5 kJ/mol for the three particle fractions. Those values are 5.2, 20 and 9.8 kJ/mol higher as compared to the corresponding FAZA particles. For zeolite-Y the E_{app} is calculated around 70–80 kJ/mol depending if all the experimental points are taken into

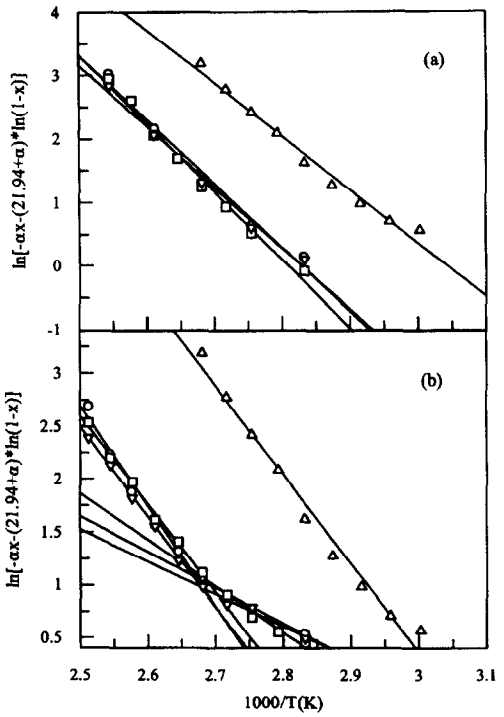

Fig. 7. Arrhenius plots for the isopropanol decomposition drawn according to Eq. (11) of the three fractions (○, 200–250 μm; □, 425–500 μm and ▽, 710–1000 μm) of AZA (a) and FAZA (b). The data for zeolite-Y are also shown for comparison (△).

account or ignoring the two lower temperature points (see Fig. 7). In this respect the lower limit behaviour of zeolite-Y is reminiscent of that of FAZA.

The question now is which is the reason for this peculiar behaviour of FAZA? We believe that this is due to an alternation of kinetics. In other words the first order kinetic Eq. (7) does not hold for the whole range of conversion. There are two possibilities here: One is that isopropanol itself is strongly adsorbed at low T and low conversions on FAZA. If so, the kinetic equation should be $R = k$ and apparent activation energy of the reaction E_{app} should equal E_{true}. However then the activation energies found at lower temperatures should be higher as compared to those found in higher temperatures as calculated by the first order Eq. (7). Clearly this is not the case. The other possibility is that water, when produced in large enough quantities at higher conversion at $T > 100$°C acts

Table 2
Activation energies on AZA, FAZA and zeolite LZ-Y62 calculated (i) from the plots of Fig. 7, and (ii) from the plots of $\ln R$ vs. $1000/T$

Sample	LZ-Y62	AZA			FAZA					
Fraction (μm)	–	200–250	425–500	710–1000	200–250		425–500		710–1000	
					Low Temp.	High Temp.	Low Temp.	High Temp.	Low Temp.	High Temp.
E_a (kJ/mol) [a]	69.7	83.8	89.5	79.9	28.1	78.6	36.5	69.5	25.2	70.7
E_a (kJ/mol) [b]	58.8	72.6	78.5	70.2	26.6	66.8	34.6	59.4	24.1	61.7

[a] 1st order kinetics (Eq. 11).
[b] From plots of $\ln R$ vs. $1000/T$.

inhibitively. Then the apparent activation energy of the reaction should appear increased by an amount equal to that of the heat of adsorption of water i.e.

$$E_{app} = E_A - \Delta H_{C_3H_8O} + \Delta H_{H_2O}$$

since at $T < 100°C$

$$E_{app} = E_A - \Delta H_{C_3H_8O}$$

In other words the difference between the two sets of activation energies on FAZA (see Table 2) which averages around 43 kJ/mol (10.2 kcal/mol) corresponds to the enthalpy of adsorption of water on the catalyst surface.

To check the above hypothesis we applied the Arrhenius treatment in the observed rate of reaction e.g. without applying 1st order or any other kinetics. So we plot the value of $\ln R$ vs. $1000/T$. The results obtained are practically similar to those found from the treatment of 1st order kinetics. In other words on AZA fractions as well as on zeolite-Y just one slope was observed in the Arrhenius lines while on FAZA we had two regions, one corresponding to $T < 100°C$ and low values of E_{app} and a second corresponding to $T > 100°C$ and higher values of E_{app}. The numerical results are included in Table 2. The important point we draw attention to, is that again the difference between the E_{app} values observed at $T > 100°C$ and the E_{app} at $T < 100°C$ is averaged to 34 kJ/mol (8.1 kcal/mol) compared to 43 kJ/mol (10.2 kcal/mol) from 1st order kinetics. So it seems that indeed there is an increment of E_{app} at higher conversions which must be due to the inhibited action of water and the difference observed 8–10 kcal/mol equals the value of ΔH_{H_2O} as observed in the past by several researchers.

The question remaining now is what is the reason for this different behaviour of FAZA compared to that of AZA solids? To be more precise, why does water appear to be more loosely bound on FAZA at low partial pressures while on AZA it is strongly bound even at minute amounts?

After several attempts we reach the conclusion that an answer to this question can be provided by examining the thermochemical equations

$$2Al(OH)_3 \rightarrow Al_2O_3 + 3H_2O \tag{12}$$

$$\Delta H_{reaction} = \Delta H_{Al_2O_3} + 3\Delta H_{H_2O(g)} - 2\Delta H_{Al(OH)_3} = +152\,kJ/mol$$

$$2Fe(OH)_3 \rightarrow Fe_2O_3 + 3H_2O \tag{13}$$

$$\Delta H_{reaction} = \Delta H_{Fe_2O_3} + 3\Delta H_{H_2O(g)} - 2\Delta H_{Fe(OH)_3} = +96 kJ/mol$$

From the above it is clear that water is more loosely bound on Fe compared to Al. For mixed systems containing both Al and Fe, according to Eq. (14) we should have

$$Al(OH)_3 \cdot Fe(OH)_3 \rightarrow AlFeO_3 + 3H_2O \tag{14}$$

$$\Delta H_{reaction} = (152 + 96)/2 = 124 kJ/mol$$

This amount of energy is needed for removing three water molecules, therefore for the removal of just one water molecule we need $124/3 = 41$ kJ/mol. This result is not actually very surprising: It matches exactly the heat of adsorption of water on FAZA that was calculated to be 43 kJ/mol on average from the three fractionated particles of it. However the same result, also points to another consequence, namely that the reaction of isopropanol dehydration actually takes place on the pillars, AlO_x in AZA and $Al_{0.5}Fe_{0.5}O_x$ in FAZA. Otherwise if the reaction did not occur on the pillars but, let us say, on the aluminosilicate surface we should not observe the variation of mechanism and of activation energies of the reaction. Perhaps this is also the reason for the differentiation of selectivities

relative to propene of AZA and FAZA as compared to zeolite-Y. It might be that the dehydration occurring on the pillars existing in the very narrow two dimensional galleries takes place from one single molecule of isopropanol. On the contrary, for zeolite-Y the dehydration in the cages, which play the role of microreactors, takes place from two isopropanol molecules to a much greater extent.

5. Conclusions

The AZA and FAZA pillared materials, prepared in the context of CEA-PLS (producer Straton Hi Tec, Ltd) are highly porous aluminosilicate solids having pillars consisted of either AlO_x or $Al_{0.5}Fe_{0.5}O_y$. They are acidic solids, their surface acid density be similar to that of zeolite-Y. Their porosity appears isomorphous in three dimension with a fractal dimensionality 2.8–3.0. Their catalytic activity relative to the isopropanol decomposition appears even at $T < 100°C$. The product at the reaction is propene with a selectivity of > 0.9 while small amounts of diisopropyl ether are also produced. For comparison zeolite-Y provides almost equal amounts of propene and diisopropyl ether. Such materials are promising in reactions necessitating acid sites like Friedel–Crafts alkylation, isomerizations and disproportionations of organic molecules.

Acknowledgements

The authors thank the Straton Hi Tec Ltd., Athens, for the generous donation of AZA and FAZA samples. This work was carried out in the context of 'Coordinated European Activity on Pillared Layered Structures' (CEA-PLS). A.L and P.T. acknowledge financial help from the STRIDE-HELLAS 33 program of the E.U. and PENED-92 program of the G.S.R.T. Various discussions with N. Gangas, N. Papayannakos, T. Bakas and A. Moukarika helped in the formulation of various aspects of this work.

References

[1] T.J. Pinnavaia, Science, 220 (1983) 365.
[2] R.M. Barrer and D.M. MacLeod, Trans. Faraday Soc., 51 (1955) 1290.
[3] H. Lahav, U. Shani and J. Shabtai, Clays Clay Miner., 26 (1978) 107.
[4] D. Plee, L. Gatineau and J.J. Fripiat, Clays Clay Miner., 35 (1987) 81.
[5] S. Shah Singh and H. Kodama, Clays Clay Miner., 36 (1988) 397.
[6] M.A. Martin-Luengo, H. Martins-Carralho, J. Ladriere and P. Grange, Clay Miner., 24 (1989) 495.
[7] G.W. Brindley and S. Yamanaka, Amer. Mineralogist, 64 (1979) 830.
[8] S. Yamanaka and G.W. Brindley, Clays and Clay Miner., 27 (1979) 119.
[9] S. Yamanaka and G.W. Brindley, Clays and Clay Miner., 26 (1978) 21.
[10] S.P. Skaribas, P.J. Pomonis, P. Grange and B. Delmon, J. Chem. Soc., Faraday Trans., 88 (21) (1992) 3217.
[11] W.Y. Lee, R.H. Raythatha and B.J. Tatarchuk, J. Catal., 115 (1989) 159.
[12] D.E.W. Vaughan and R.J. Lussier, in L.V. Rees (Ed.), Proc. 5th Int. Conf. Zeolites, Heyden, London, 1980, p. 94.
[13] CEA-PLS. For more details contact H. Van Damme (Coordinator) CNRS/CROCSI.
[14] Pillared Layered Stuctures, in I. Mitchell (Ed.), Elsevier Applied Science, London, 1990.
[15] D.E. Petrakis, P.J. Pomonis and A.T. Sdoukos, J. Chem. Soc., Faraday Trans., 87 (9) (1991) 1439.
[16] A.K. Ladavos and P.J. Pomonis, Stud. Surf. Sci. Catal., 63 (1991) 319.
[17] C. Ancion and G. Poncelet, Appl. Catal., A, 108 (1994) 31.
[18] M. Lennarda, R. Ganzerla, R. Zanoni, S. Enzo and L. Storaro, J. Mol. Catal., 92 (1994) 201.

[19] T. Bakas, A. Moukarika and N.H. Gangas, paper presented at 'Athens '94 CEA-PLS Meeting on Reference PILCs', 18 and 19 November 1994.
[20] S.J. Gregg and K.S.W. Sing, Adsorption, Surface Area and Porosity, Academic Press, New York, 1982, p. 98.
[21] J. Seifert and G. Emig, Int. Chem. Eng., 31 (1991) 29.
[22] V.V. Yushchenko, A.N. Zakharov and B.V. Romanovskii, Kinet. Catal., 27 (1986) 409.
[23] B.B. Mandelbrot (Ed.), The Fractal Geometry of Nature, Freeman, San Francisco, CA, 1992.
[24] D. Farin and D. Avnir, The Fractal Nature of Molecule – Surface Interactions and Reactions, Ch. 4.12. in D. Avnir (Ed.), The Fractal Approach to Heterogeneous Chemistry – Surfaces, Colloids, Polymers, J. Wiley and Sons, Chichester, 1989.
[25] D. Avnir, D. Farin and P. Pfeifer, New J. Chem., 16 (1992) 439.
[26] H. Van Damme and J.J. Fripiat, J. Phys. Chem., 82 (1985) 2785.
[27] M. Ben-Ohoud and H. Van Damme, C.R. Acad. Sci. Paris, Ser. II, 311 (1990) 665.
[28] F. Pepe, C. Angelleti, S. DeRossi and M. LoJacono, J. Catal., 91 (1985) 69.
[29] K. Balasubramanian and V. Krishnasan, J. Chem. Soc., Faraday Trans. 1, 82 (1986) 2265.
[30] M. Richter and G. Ohlmann, Appl. Catal., 36 (1988) 81.
[31] A. La Ginestva, P. Patrono, M.L. Benardelli, P. Galli, C. Ferragina and M.A. Massucci, J. Catal., 103 (1987) 346.
[32] B.Z. Wan, R.G. Antony, G.Z. Pery and A. Clearfield, J. Catal., 101 (1986) 19.
[33] A.K. Ladavos and P.J. Pomonis, J. Chem. Soc., Faraday Trans., 87 (19) (1991) 3291.
[34] A.K. Ladavos and P.J. Pomonis, J. Chem. Soc., Faraday Trans., 88 (17) (1992) 2557.